OPEN

Tissue-specific mechanical and geometrical control of cell viability and actin cytoskeleton alignment

Dong Wang[1,2], Wenfu Zheng[1], Yunyan Xie[1,2], Peiyuan Gong[1], Fang Zhao[1], Bo Yuan[1,2], Wanshun Ma[1], Yan Cui[1], Wenwen Liu[1,2], Yi Sun[1,2], Matthieu Piel[3], Wei Zhang[1] & Xingyu Jiang[1]

[1]Beijing Engineering Research Center for BioNanotechnology & CAS Key Lab for Biological Effects of Nanomaterials and Nanosafety, National Center for Nanoscience and Technology, 11 Beiyitiao, ZhongGuanCun, Beijing 100190, China, [2]Graduate University of the Chinese Academy of Sciences, Beijing 100846, China, [3]Biologie du cycle cellulaire et de la motilité, CNRS, Institut Curie, 26 rue d'Ulm 75248 Paris Cedex 05, France.

Different tissues have specific mechanical properties and cells of different geometries, such as elongated muscle cells and polygonal endothelial cells, which are precisely regulated during embryo development. However, the mechanisms that underlie these processes are not clear. Here, we built an *in vitro* model to mimic the cellular microenvironment of muscle by combining both mechanical stretch and geometrical control. We found that mechanical stretch was a key factor that determined the optimal geometry of myoblast C2C12 cells under stretch, whereas vascular endothelial cells and fibroblasts had no such dependency. We presented the first experimental evidence that can explain why myoblasts are destined to take the elongated geometry so as to survive and maintain parallel actin filaments along the stretching direction. The study is not only meaningful for the research on myogenesis but also has potential application in regenerative medicine.

A core question in developmental biology is how cell shape is regulated during tissue morphogenesis. There are different types of cells in different tissues and the specific cell shapes are closely related to their functions. For example, epithelial or endothelial cells are polygonal and have complex cell-cell junctions forming a continuous sheet that functions as a barrier and allows for selective transportation. Neurons have radiated shapes with dendrites and axons that form neural networks transmitting electrical and biochemical signals. Muscle cells have elongated shapes forming muscle fibers that transmit mechanical force. However, little is known why muscle cells would take such unique shapes among dozens of possible choices.

In recent years, extracellular microenvironment has been reported to play important roles in regulating the functions of the cells. For example, substrate stiffness can influence the focal adhesion, cytoskeleton assembly, spreading and differentiation of the cells[1]. Cells can also sense the topography or geometry of the substrate and align their major axes by contact guidance[2,3], and change their cytoskeleton alignment[4], traction force[5], proliferation[6,7] or differential potential[8]. Mechanical force is an important factor that regulates embryo development and tissue morphogenesis, especially in musculoskeletal tissues[9,10]. For *in vitro* experiments, elastic membranes were used in many models to mimic mechanical stretch to the cells[11–14]. While being stretched on elastic membranes along uniaxial direction, the cells would change their shapes and align their major axes and actin filaments (F-actin) perpendicular to the direction of stretch[15–21]. The shapes with major axes parallel to the direction of stretch were thought to be unstable based on the *in vitro* studies on smooth muscle cells, endothelial and epithelial cells[15–21]. However, questions arise when we think of the *in vivo* natural shapes of muscle cells[22], which actually have elongated shapes and experience mechanical stretch along their major axes. They also have stable F-actin along the stretching direction, which cannot be well explained by current *in vitro* experimental and theoretical models. We hypothesize that, in addition to genetic and biochemical regulation, physical factors including cell geometry and mechanical stretch also play an active role during myogenesis.

The techniques of soft lithography make it possible to manipulate single cells *in vitro*[23]. In this article, we built an *in vitro* model by patterning single myoblast C2C12 cells (muscle progenitor cells), along with human umbilical vascular endothelial cells (HUVECs) and NIH 3T3 fibroblasts for comparison, to different rectangular geometries and applied mechanical stretch along their major axes to mimic the mechanical microenvironment of muscle cells

in vivo. A stretching system was developed to image the real-time dynamics of single actin filaments in living cells during stretching[13].

Results

Patterning single cells on the stretching device. The stretching device was manufactured as reported before[13] (Figure 1, A–B). The method for patterning single cells on the elastic polydimethylsiloxane (PDMS) membrane of the device was modified from Nelson *et al.* (2003)[24] and Mayer *et al.* (2004)[25] (Figure 1, C). We chose the areas from 500 to 4000 μm^2, after examining the spreading areas of the three types of cells (C2C12, HUVEC and 3T3) without confinement on PDMS membranes (see Supplementary Figure S1 and Table S1 online). Using agarose gel stamp and microcontact printing, we got stable single-cell patterning on PDMS membranes (Figure 1, D and Supplementary Figure S2 online). We referred to "40 μm × 50 μm" as "40 × 50", and so on hereafter. It was hard for HUVEC and 3T3 cells to occupy the whole area of 10 × 400, which were not included in the data analysis.

Geometrical control of cell viability under stretch. The cells were cultured in the stretching device overnight and then used for experiment. Propidium iodide was added to the culture medium for detecting dead cells. All the cells were monitored for at least 10 min before stretching and we didn't find any cell death in all the experiments. After 10 min of cyclic uniaxial mechanical stretch, almost all the HUVECs on all the geometries survived (Figure 2, A). The 3T3 cells on most of the geometries survived, except those of 40 × 75 and 40 × 100 with the survival ratio of around 60% (Figure 2, B). However, it was very interesting that the viability of C2C12 cells under stretch was highly dependent on geometry (Figure 2, C):

(1)   The C2C12 cells of 10 μm width had the highest viability, independent on spreading areas;

(2)   Given the same areas, the thinner C2C12 cells had higher viability than the wider ones;

(3)   Given the same widths, the smaller cells had higher viability than the larger ones.

As actin cytoskeleton is the main cellular architecture responsible for transducing mechanical forces[26], we next investigated the possible role of F-actin in this geometrical dependence of viability. We chose the shape of 40 × 100, which had the lowest viability for C2C12 cells under stretch. Blebbistatin (50 μM) was added to the culture medium to inhibit myosin II and lower the tension of cytoskeleton during stretch, which rescued about half of the C2C12 cells from death
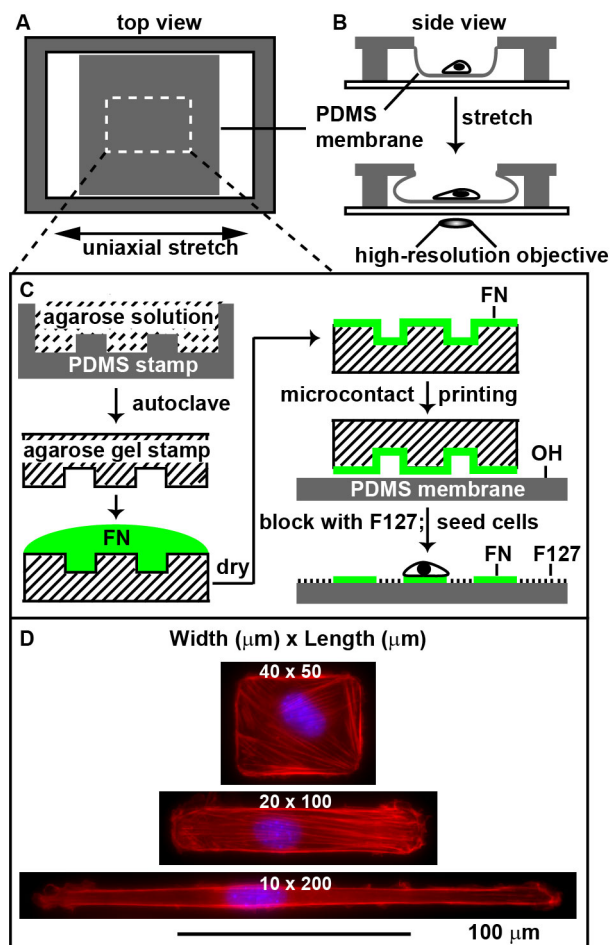

Figure 1 | Top (A) and side (B) views of the stretching device. Single cells were confined in specific geometries on the elastic membranes (white dashed rectangle) by microcontact printing using agarose stamp (C). Fibronectin (FN, green) was used to promote cell adhesion and Pluronic F127 was used as the blocking molecule. Single C2C12 cells of 2000 μm^2 (40 × 50, 20 × 100 and 10 × 200) were successfully confined in different shapes (blue, nuclear stained by DAPI; red, F-actin stained by Rhodamine Phalloidin) (D). The entire list of the geometries of C2C12 cells can be found as Supplementary Figure S2 online.
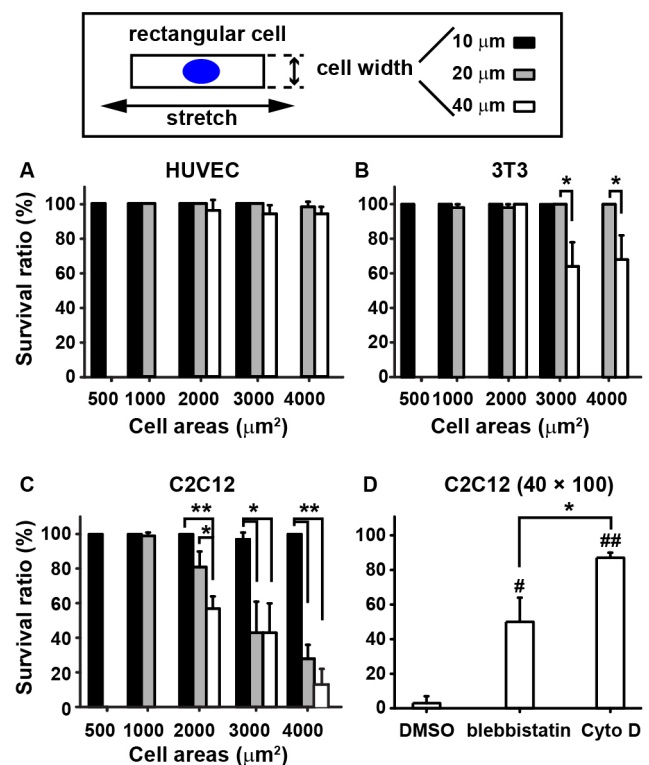

Figure 2 | Single cells of the three types were patterned in the rectangular geometries listed in Supplementary Table S1 and stretched for 10 min. Almost all the HUVECs survived the stretch (A). Most of the 3T3 cells maintained good viability, except those with the width of 40 μm and areas larger than 2000 μm^2 (B). The viability of C2C12 cells were highly dependent on their geometries (C): almost all the C2C12 cells of 10 μm width survived stretch; given the same areas, thinner cells had higher viability; given the same widths of 20 or 40 μm, smaller cells had higher viability. Reducing the tension of actin cytoskeleton by blebbistatin or Cyto D rescued the C2C12 cells of 40 × 100 (D). The black, grey and white bars represent the geometries of 10, 20 and 40-μm widths respectively. * and **, significant difference (*, $P < 0.05$; **, $P < 0.01$) between groups; # and ##, significant difference (#, $P < 0.05$; ##, $P < 0.01$) from DMSO.

(Figure 2, D). By disassembling F-actin with cytochalasin D (Cyto D, 1 μM), which stayed in the culture medium during the stretching experiments, we further increased the survival ratio to above 80% (Figure 2, D). The results indicated that actin cytoskeleton played a key role in the geometrical regulation of cell viability under mechanical stretch. To investigate how actin cytoskeleton responds to cell geometry and mechanical stretch, we next used confocal microscopy to image the real-time F-actin dynamics of single C2C12 cells under stretch.

Cell area, not the length of F-actin, determines the stability of peripheral F-actin of C2C12 cells under stretch. We chose the geometries of smaller areas: 500, 1000 and 2000 μm² for real-time F-actin study because of the higher viability of C2C12 cells on these geometries (Figure 2, C). The C2C12 cells were transiently transfected with the plasmid that encodes Lifeact-mcherry[27,28] and the F-actin would be labeled with mcherry. The positive cells were sorted by flow cytometry and used for experiments. As reported before, we found that F-actin alignment was dependent on the cell geometry in static conditions[4]. In the rectangular cells of different geometries, there were peripheral thick F-actin bundles along the longest sides of the rectangles and thin F-actin fibers in the center, which were referred to as "peripheral F-actin" and "central F-actin" respectively (Figure 3, A). As actin cytoskeleton has a three-dimensional (3D) architecture in the cell body[29–31], the definition of "peripheral F-actin" and "central F-actin" here was based on two-dimensional (2D) view of the cell[20,32]. The states of F-actin were classified into two groups: intact F-actin, which had continuous and tensioned morphology; broken F-actin, which was broken into pieces and disassembled by parallel stretch (Figure 3, B). Dozens of cells were counted for calculating the ratios of the cells with intact F-actin (Figure 3 and Supplementary Table S2 online). For the control study, we captured the images of the cells at least 10 min before stretch and found no obvious change of F-actin.

We first examined the dynamics of peripheral F-actin of C2C12 cells under stretch. The cells of the same lengths were compared on the stability of peripheral F-actin after stretch. The cells with intact peripheral F-actin after stretch were counted for analysis. In each group with the length of 50 or 100 μm, the peripheral F-actin of the thinner cells had higher stability than those of the wider ones (Figure 3, C), although the cells in each group had the similar lengths of F-actin. The result indicates that it is cell area, not the length of F-actin, that determines the mechanical properties of actin filaments. There may be different molecular components of the actin stress fibers in the cells of different areas.

Cell shape guides central F-actin reassembly of C2C12 cells under stretch. The central F-actin was classified into two groups: parallel central F-actin, having the angle with stretching direction less than 45°; perpendicular central F-actin having the angle larger than 45°. In the C2C12 cells with the widths of 20 and 40 μm, most of the parallel central actin filaments were broken and disassembled; there were stable perpendicular central actin filaments after stretch (Figure 3, D and E). This result is consistent with the published reports that uniaxial mechanical stretch induces actin filaments to reassemble and align along the perpendicular direction[15–21].

It was very interesting that there was new parallel central F-actin assembly in the C2C12 cells of 10 × 100 (25%, 14 of 57 cells) (Figure 3, E). The regulating role of cell geometry on cytoskeleton under stretch is well illustrated in the C2C12 cells of 10 × 100 and 20 × 50 (Figure 4 and Supplementary Figure S3 online). Although they have the same area, different cell shapes lead to different F-actin alignments. This result cannot be well explained by current experiment models or theories[15–21], but it is consistent with the *in vivo* natural shapes of muscle cells[22].

Discussion
We found that myoblast C2C12 cells were more sensitive to geometries than endothelial cells (HUVECs) or fibroblasts NIH 3T3
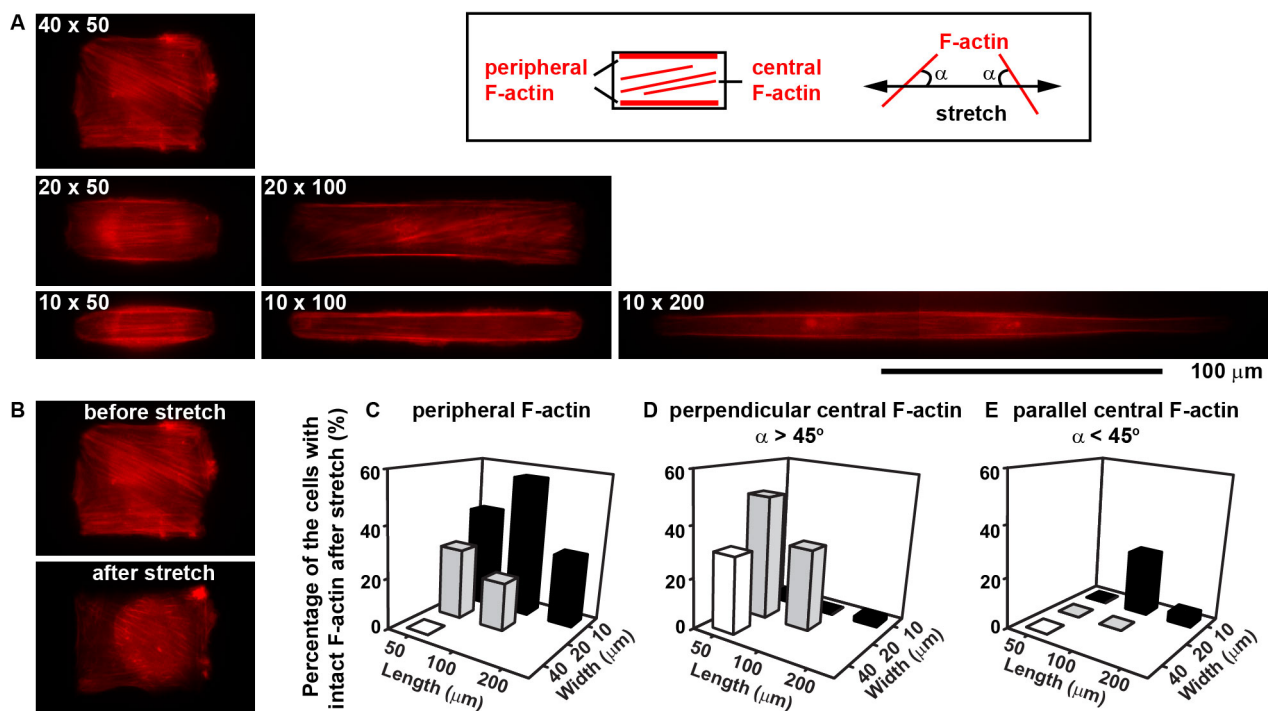

Figure 3 | F-actin (red) alignment of C2C12 cells with different geometries (A). There are two types of actin filaments: peripheral and central F-actin (A). After stretch, the actin filaments of some cells were broken into pieces and disassembled (B). The percentage of the cells that had intact actin filaments after stretch was calculated: (C), peripheral F-actin; (D) perpendicular central F-actin; (E), parallel central F-actin. "α" is defined as the angle between central F-actin and stretching direction. Parallel central F-actin has the angle α < 45°; perpendicular central F-actin has the angle α > 45°.
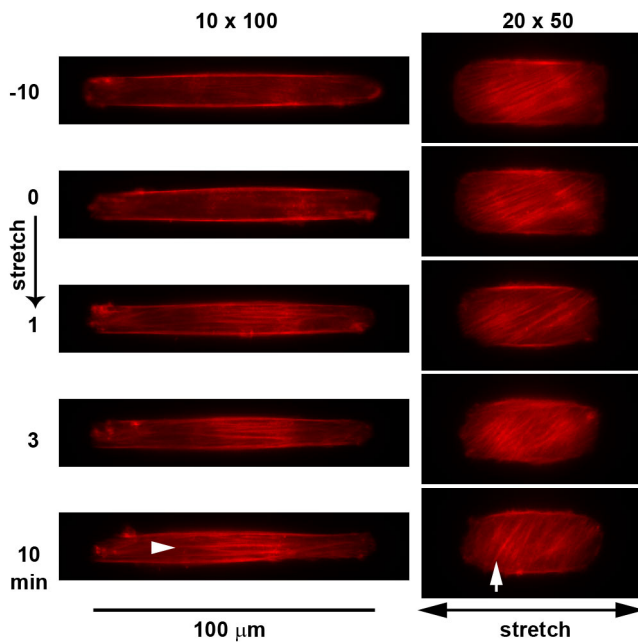
Figure 4 | Real-time F-actin (red, Lifeact-mcherry) dynamics of the C2C12 cells of 10 × 100 and 20 × 50 under stretch. The newly formed central F-actin in the C2C12 cell of 10 × 100 aligned parallel to stretching direction (arrowhead); however the new central F-actin of the C2C12 cells of 20 × 50 aligned perpendicular to stretching direction (arrow). See Supplementary Figure S3 online for more examples.

considering cellular viability under mechanical stretch (Figure 2, A–C). Among all the geometries tested in the experiments, the thinnest 10-µm wide ones rendered C2C12 cells highest viability, which is consistent with the natural shapes of muscle cells[22].

It was very interesting that HUVECs and 3T3 fibroblasts didn't have such geometrical effect under stretch. They had higher viability than C2C12 cells even with the spreading area of 4000 µm² (Figure 2, A–C). However, in a similar study about geometrical control of cell growth without mechanical stimuli, capillary endothelial cells grew better on larger spreading areas, but underwent apoptosis on smaller ones[7]. The both results confirm the idea that microenvironment plays important roles in regulating cellular activities[1,3]. Different tissues have different physical and biochemical microenvironments and the cells of them have specific cytoskeleton architectures and regulatory mechanisms. In this regard, it is quite understandable that HUVECs didn't show such geometrical effect under stretch. One possible reason for HUVECs survival under stretch might be vascular endothelial growth factor (VEGF). VEGF is a survival factor for vascular endothelial cells both *in vivo* and *in vitro*. It is needed for the *in vitro* culture of vascular endothelial cells[33–35]. Mechanical stimuli and VEGF are closely related in vascular endothelial cells. Mechanical stimuli, such as cyclic stretch and shear stress, can upregulate VEGF and VEGF receptor 2 expression of vascular endothelial cells, and can protect endothelial cells from apoptosis through VEGF pathway. Knocking down VEGF or Blocking VEGF receptor led to increased apoptosis of HUVECs under shear stress[36,37]. VEGF might also play an important role as a survival factor in the stretching experiment, as it does under flow shear stress[37], forming a positive feedback loop between vascular endothelial cells and mechanical stimuli. On the other hand, vascular endothelial cells mainly experience flow shear stress, hydraulic pressure and small mechanical strain, and they also need a larger spreading area to form the inner lining of blood vessels. They have advanced cell-cell junctions and cell-extracellular matrix connections which mediate most of the mechanical forces. However there is no cell-cell junction in the

single-cell experiments, which might be one of the reasons why endothelial cells didn't respond to cell geometry and mechanical stretch in our system. On the contrary, mechanical stretch is the main physical factor in muscle tissues and cytoplasmic actin filaments are the main structures that transduce external mechanical stretch and produce force by the specialized actin-myosin architecture in muscle cells, which makes them highly sensitive to stretch. After adding blebbistatin or Cyto D to reduce the tension of actin stress fibers or completely disassemble actin filaments, the viability of wider C2C12 cells increased and the geometrical dependence tended to disappear (Figure 2, D). This confirms that actin cytoskeleton is a key factor that mediates the geometrical dependence on mechanical stretch.

Inhibition of intracellular actomyosin tension by blebbistatin or Cyto D has been reported to induce the disassembly of actin filaments and focal adhesions and block cell proliferation[38,39]. However, this effect of actomyosin tension on cell proliferation can be reversed by modulating extracellular physical microenvironment. By modulating the extracellular matrix stiffness, Mih *et al.* found that blebbistatin could promote fibroblast proliferation on soft matrix[40]. Cyto D was reported to have a tissue-specific function by promoting cell survival in serum-starved fibroblast, but not mesangial cells, by activation of gelatinase A[41]. In a recent report, total gelatinase activity was increased in C2C12 cells, but not in fibroblasts, under mechanical stretch[42]. Our results indicate that the extracellular physical factors play important roles in regulating cell behavior, in a tissue-specific manner. Tissue-specific cellular microenvironment should be considered in the future study of mechanotransduction.

To further investigate how actin cytoskeleton responds to mechanical stretch in a cellular geometrical dependent manner, we transfected C2C12 cells with the plasmid that encodes Lifeact-mcherry, which was reported to bind to F-actin and have few interference on its normal function[27,28]. We investigated two kinds of actin filaments: peripheral and central F-actin, as they were reported to be regulated by different mechanisms[20,32]. We found that thinner cells had higher stability of peripheral F-actin than wider ones, even given the same areas (Figure 3, A, C). It was very interesting that the peripheral actin filaments in the cells of different geometries had different mechanical properties even they had the same lengths. For example, among the three geometries in the 50-µm length group, or the two in the 100-µm group, 10-µm width was the best one that rendered C2C12 cells the most stable peripheral F-actin. This confirmed again the results of viability assay (Figure 2) that thinner C2C12 cells have not only higher viability but also more stable peripheral F-actin.

The result of central F-actin in wider (20 and 40-µm width) C2C12 cells are consistent with the reports that uniaxial mechanical stretch induces actin filaments reassemble and align along the perpendicular direction of stretch[15–21]. However, it is very interesting that the narrow 10-µm geometry can force actin filaments to reassemble, but on the contrary, along the direction of stretch (Figure 3, D and E). The regulating role of cell shape on F-actin alignment is well illustrated in the C2C12 cells of 10 × 100 and 20 × 50, even though they have the same spreading area (Figure 4). The realignment process happened in 10 min, indicating the fast response of myoblasts to extracellular physical microenvironment (Figure 4).

The peripheral and central actin filaments were reported to be regulated by different molecular pathways: the peripheral F-actin mainly depends on myosin light chain kinase (MLCK), while central F-actin was mainly dependent on Rho-kinase[20,32]. Lee *et al.* applied cyclic uniaxial stretch to the cells treated with Rho-kinase inhibitor Y27632 and found that central F-actin disappeared and there was thick peripheral F-actin after stretch[20]. On the contrary, inhibiting MLCK by ML-7 led to disappearance of peripheral F-actin and formation of central F-actin parallel to the stretching direction[20]. In our experiment, thinner cells have higher stability of peripheral F-actin, which is similar to the effect of Rho-kinase inhibitor; the

geometry of 10×100 can also induce parallel central F-actin formation along the stretching direction, which is similar to the effect of MLCK inhibitor[20]. Further study is needed to investigate the relationship between cell geometry and the activities of Rho-kinase and MLCK under stretch.

Here we studied the actin cytoskeleton dynamics under geometrical and mechanical regulation from the 2D view. However, the actin cytoskeleton has a 3D architecture, which can form dorsal and ventral F-actin and transverse arcs[29]. More importantly, F-actin can form a perinuclear cap around the nucleus, which directly regulates nuclear shape and plays important roles in mechanotransduction[30,31,43]. Further studies are needed to investigate the 3D dynamics of actin cytoskeleton under geometrical and mechanical stimuli. Focal adhesions mediate the cell-extracellular matrix (ECM) interaction and transduce forces between each other[44,45]. It is also very interesting to study the dynamics of focal adhesions in this geometrical and mechanical system. For this purpose, a better patterning method for controlling ligands density on soft membranes should be developed.

In summary, we, for the first time, presented the experimental evidence that the elongated geometry can render myoblast C2C12 cells optimal viability under stretch and the most stable actin filaments parallel to the direction of stretch, which are the prerequisites for the normal functions of muscle cells. In the *in vivo* microenvironment of skeletal muscle, myoblasts reside in a compact space full of mechanical stretch, where they have to take the elongated shape along the stretching direction, so that they can first survive and next start the differentiation and fusion processes. The methods provided in this report, together with others, will help us understand how a single cell is regulated by the microenvironment, which is not only meaningful to the basic research of embryo development and morphogenesis, but also has potential application in tissue engineering and regenerative medicine.

Methods

Cell culture and transfection. NIH 3T3 and C2C12 cells were cultured in Dulbecco's modified Eagle's medium (DMEM, Invitrogen) supplemented with 10% fetal bovine serum (FBS, Gibco), 1 mM L-glutamine (Gibco), 100 U/ml penicillin (Gibco), and 100 mg/ml streptomycin (Gibco). Primary HUVECs were isolated from human umbilical cords and cultured in M199 (Invitrogen) supplemented with 20% FBS, 1 mM L-glutamine, 100 U/ml penicillin, 100 mg/ml streptomycin and 10 ng/ml vascular endothelial growth factor (Invitrogen). HUVECs were used between second and third passages. All the cells were cultured in a humidified 5% CO_2 incubator at 37°C. C2C12 cells were transfected with the plasmid of Lifeact-mcherry, by the reagent of Lipofectamine™ LTX (Invitrogen). The positive cells were sorted by flow cytometry (FACSVantage Diva, Becton, Dickinson and Company, BD).

Patterning single cells on the stretching device. The patterning method in this paper (Fig. 1, C) was modified from the methods of Nelson et al. (2003)[24] and Mayer et al. (2004)[25]. The reversed polydimethylsiloxane (PDMS, Dow Corning, Sylgard 184) stamp was made by soft lithography. We made a chamber on the PDMS stamp, added agarose powder (N605, Amresco) and distilled water in the chamber to the final agarose concentration of 8% and sterilized it at 121°C for 20 min in an autoclave. When taken out of the autoclave, the agarose solution cooled down and gelated at room temperature naturally. We obtained the agarose stamp after gently peeling the agarose gel off the reversed PDMS stamp. The agarose stamp was cut to a proper size, incubated with 50 μg/ml fibronectin (FN, BD) solution in phosphate buffered saline (PBS) for about 5 min, allowed to dry naturally and printed on the PDMS membrane of the stretching device, which was pretreated with air plasma (Weike, PDC-MG). After about 5 min of conformal contact, we peeled off the agarose stamp and blocked the substrate with 0.2% Pluronic F127 (Invitrogen) solution in PBS for at least 1 h, before seeding cells (Fig. 1, C).

Application of mechanical stretch. The cells were cultured overnight and then stimulated by 30% uniaxial stretch at the frequency of 0.5 Hz along the major axes of the cells for 10 min. In the experiments of viability, we added propidium iodide (PI, Invitrogen) to the culture medium with the final concentration of 4 μM to identify the dead cells. PI was in the culture medium throughout the stretch experiments. In the experiments of inhibiting the tension of F-actin, the cells were treated with 50 μM blebbistatin (Sigma) and 1 μM Cyto D (Sigma) for 1 h before stretch. The inhibiting reagents remained in the culture medium throughout the stretch experiments. In the experiments of real-time F-actin dynamics of C2C12 cells, the culture medium was changed to DMEM containing no phenol red (Invitrogen) with 5% FBS at 37°C before stretch.

Microscopy and data analysis. The cells were viewed on a Leica DMI6000 inverted microscope with a 63× oil objective for cell viability experiment and an Olympus FV1000 confocal microscope with a 63× oil objective for F-actin imaging. The objective stage of the microscope was warmed to 37°C during experiments. The calibration was done in each device after the stretch. The data were collected from the devices which had the stretch magnitudes of 30 ± 3%. Data analysis was performed by Adobe Photoshop, Adobe Illustrator, Image Pro Plus and Origin. In the experiments of viability, we captured the images of the cells at two time points: −10 and 0 min, as control before applying stretch, applied cyclic uniaxial stretch for 10 min, and captured the images of the cells after stretch. For each type of the cell on each geometry, there were 3 repeats of stretching, at least 10 cells for each repeat, except that there were at least 5 cells for each repeat of 10×300, and a total cell number of at least 10 cells for C2C12 cells of 10×400. Results were expressed as mean ± SD. Student's *t*-test was used to compare two groups. * and # indicate significant difference of $P < 0.05$. ** and ## indicate significant difference of $P < 0.01$. In the experiments of real-time F-actin dynamics of C2C12 cells, the total cell number was at least 20 for each shape. We captured the images of F-actin at −10 and 0 min as control before stretch, and after 1, 3 and 10 min of stretch.

1. Discher, D. E., Janmey, P. & Wang, Y. L. Tissue cells feel and respond to the stiffness of their substrate. *Science* **310**, 1139–1143 (2005).
2. Jiang, X. Y. et al. Controlling mammalian cell spreading and cytoskeletal arrangement with conveniently fabricated continuous wavy features on poly(dimethylsiloxane). *Langmuir* **18**, 3273–3280 (2002).
3. Vogel, V. & Sheetz, M. Local force and geometry sensing regulate cell functions. Nat. Rev. *Mol. Cell Biol.* **7**, 265–275 (2006).
4. Thery, M., Pepin, A., Dressaire, E., Chen, Y. & Bornens, M. Cell distribution of stress fibres in response to the geometry of the adhesive environment. *Cell Motil. Cytoskeleton* **63**, 341–355 (2006).
5. Lemmon, C. A. & Romer, L. H. A Predictive Model of Cell Traction Forces Based on Cell Geometry. *Biophys. J.* **99**, L78–L80 (2010).
6. Thakar, R. G. et al. Cell-Shape Regulation of Smooth Muscle Cell Proliferation. *Biophys. J.* **96**, 3423–3432 (2009).
7. Chen, C. S., Mrksich, M., Huang, S., Whitesides, G. M. & Ingber, D. E. Geometric control of cell life and death. *Science* **276**, 1425–1428 (1997).
8. Kilian, K. A., Bugarija, B., Lahn, B. T. & Mrksich, M. Geometric cues for directing the differentiation of mesenchymal stem cells. *Proc. Natl. Acad. Sci. U. S. A.* **107**, 4872–4877 (2010).
9. Discher, D. et al. Biomechanics: cell research and applications for the next decade. *Ann. Biomed. Eng.* **37**, 847–859 (2009).
10. Li, S., Guan, J. L. & Chien, S. Biochemistry and biomechanics of cell motility. *Annu. Rev. Biomed. Eng.* **7**, 105–150 (2005).
11. Brown, T. D. Techniques for mechanical stimulation of cells in vitro: a review. *J. Biomech.* **33**, 3–14 (2000).
12. Sotoudeh, M., Jalali, S., Usami, S., Shyy, J. Y. & Chien, S. A strain device imposing dynamic and uniform equi-biaxial strain to cultured cells. *Ann. Biomed. Eng.* **26**, 181–189 (1998).
13. Wang, D. et al. A stretching device for imaging real-time molecular dynamics of live cells adhering to elastic membranes on inverted microscopes during the entire process of the stretch. *Integr. Biol.* **2**, 288–293 (2010).
14. Kurpinski, K., Chu, J., Hashi, C. & Li, S. Anisotropic mechanosensing by mesenchymal stem cells. *Proc. Natl. Acad. Sci. U. S. A.* **103**, 16095–16100 (2006).
15. Dartsch, P. C. & Betz, E. Response of cultured endothelial cells to mechanical stimulation. *Basic Res.Cardiol.* **84**, 268–281 (1989).
16. Hayakawa, K., Hosokawa, A., Yabusaki, K. & Obinata, T. Orientation of Smooth Muscle-Derived A10 Cells in Culture by Cyclic Stretching: Relationship between Stress Fiber Rearrangement and Cell Reorientation. *Zool. Sci.* **17**, 617–624 (2000).
17. Hayakawa, K., Sato, N. & Obinata, T. Dynamic reorientation of cultured cells and stress fibers under mechanical stress from periodic stretching. *Exp. Cell Res.* **268**, 104–114 (2001).
18. Kaunas, R., Nguyen, P., Usami, S. & Chien, S. Cooperative effects of Rho and mechanical stretch on stress fiber organization. *Proc. Natl. Acad. Sci. U. S. A.* **102**, 15895–15900 (2005).
19. Kaunas, R. & Hsu, H. J. A kinematic model of stretch-induced stress fiber turnover and reorientation. *J. Theor. Biol.* **257**, 320–30 (2009).
20. Lee, C. F., Haase, C., Deguchi, S. & Kaunas, R. Cyclic stretch-induced stress fiber dynamics – Dependence on strain rate, Rho-kinase and MLCK. *Biochem. Biophys. Res. Commun.* **401**, 344–349 (2010).
21. Wang, J. H. C., Goldschmidt-Clermont, P., Wille, J. & Yin, F. C. P. Specificity of endothelial cell reorientation in response to cyclic mechanical stretching. *J. Biomech.* **34**, 1563–1572 (2001).
22. Cooper, G. M. *The Cell: A Molecular Approach. 2nd edition*. Sunderland (MA): Sinauer Associates. 447 (2000).
23. Whitesides, G. M., Ostuni, E., Takayama, S., Jiang, X. Y. & Ingber, D. E. Soft lithography in biology and biochemistry. *Annu. Rev. Biomed. Eng.* **3**, 335–373 (2001).
24. Nelson, C. M., Raghavan, S., Tan, J. L. & Chen, C. S. Degradation of micropatterned surfaces by cell-dependent and -independent processes. *Langmuir* **19**, 1493–1499 (2003).

25. Mayer, M., Yang, J., Gitlin, I., Gracias, D. H. & Whitesides, G. M. Micropatterned agarose gels for stamping arrays of proteins and gradients of proteins. *Proteomics* **4**, 2366–2376 (2004).

26. Pollard, T. D. & Cooper, J. A. Actin, a Central Player in Cell Shape and Movement. *Science* **326**, 1208–1212 (2009).

27. Riedl, J. *et al.* Lifeact: a versatile marker to visualize F-actin. *Nat. Methods* **5**, 605–607 (2008).

28. Deibler, M., Spatz, J. P. & Kemkemer, R. Actin Fusion Proteins Alter the Dynamics of Mechanically Induced Cytoskeleton Rearrangement. *PLoS ONE* **6**, e22941 (2011).

29. Hotulainen, P. & Lappalainen, P. Stress fibers are generated by two distinct actin assembly mechanisms in motile cells. *J. Cell Biol.* **173**, 383–394 (2006).

30. Khatau, S. B. *et al.* A perinuclear actin cap regulates nuclear shape. *Proc. Natl. Acad. Sci. U. S. A.* **106**, 19017–19022 (2009).

31. Chambliss, A. B. *et al.* The LINC-anchored actin cap connects the extracellular milieu to the nucleus for ultrafast mechanotransduction. *Sci. Rep.* **3**, 1087 (2013).

32. Katoh, K., Kano, Y., Amano, M., Kaibuchi, K. & Fujiwara, K. Stress fiber organization regulated by MLCK and Rho-kinase in cultured human fibroblasts. *Am. J. Physiol. Cell Physiol.* **280**, C1669–1679 (2001).

33. Gerber, H. P. *et al.* Vascular endothelial growth factor regulates endothelial cell survival through the phosphatidylinositol 3′-kinase/Akt signal transduction pathway. Requirement for Flk-1/KDR activation. *J. Biol. Chem.* **273**, 30336–30343 (1998).

34. Gerber, H. P., Dixit, V. & Ferrara, N. Vascular endothelial growth factor induces expression of the antiapoptotic proteins Bcl-2 and A1 in vascular endothelial cells. *J. Biol. Chem.* **273**, 13313–13316 (1998).

35. Ferrara, N., Gerber, H. P. & LeCouter, J. The biology of VEGF and its receptors. *Nat. Med.* **9**, 669–676 (2003).

36. Zheng, W., Christensen, L. P. & Tomanek, R. J. Differential effects of cyclic and static stretch on coronary microvascular endothelial cell receptors and vasculogenic/angiogenic responses. *Am. J. Physiol. Heart Circ. Physiol.* **295**, H794–800 (2008).

37. dela Paz, N. G., Walshe, T. E., Leach, L. L., Saint-Geniez, M. & D'Amore, P. A. Role of shear-stress-induced VEGF expression in endothelial cell survival. *J. Cell Sci.* **125**, 831–843 (2012).

38. Böhmer, R. M., Scharf, E. & Assoian, R. K. Cytoskeletal integrity is required throughout the mitogen stimulation phase of the cell cycle and mediates the anchorage-dependent expression of cyclin D1. *Mol. Biol. Cell* **7**, 101–111 (1996).

39. Straight, A. F. *et al.* Dissecting temporal and spatial control of cytokinesis with a myosin II Inhibitor. *Science* **299**, 1743–1747 (2003).

40. Mih, J. D., Marinkovic, A., Liu, F., Sharif, A. S. & Tschumperlin, D. J. Matrix stiffness reverses the effect of actomyosin tension on cell proliferation. *J. Cell Sci.* **125**, 5974–5983 (2012).

41. Ailenberg, M. & Silverman, M. Cytochalasin D disruption of actin filaments in 3T3 cells produces an anti-apoptotic response by activating gelatinase A extracellularly and initiating intracellular survival signals. *Biochim. Biophys. Acta.* **1593**, 249–258 (2003).

42. Cha, M. C. & Purslow, P. P. The activities of MMP-9 and total gelatinase respond differently to substrate coating and cyclic mechanical stretching in fibroblasts and myoblasts. *Cell Biol. Int.* **34**, 587–591 (2010).

43. Wang, N., Tytell, J. D. & Ingber, D. E. Mechanotransduction at a distance: mechanically coupling the extracellular matrix with the nucleus. *Nat. Rev. Mol. Cell Biol.* **10**, 75–82 (2009).

44. Geiger, B. & Bershadsky, A. Assembly and mechanosensory function of focal contacts. *Curr. Opin. Cell Biol.* **13**, 584–592 (2001).

45. Fraley, S. I. *et al.* A distinctive role for focal adhesion proteins in three-dimensional cell motility. *Nat. Cell Biol.* **12**, 598–604 (2010).

Acknowledgments

Author contributions

D.W. and X.J. conceived the study. D.W. and X.J. designed the experiments. D.W., W.Z., Y.X., P.G., F.Z., B.Y., W.M., Y.C., W.L. and Y.S. performed the experiments. M.P. provided the plasmid. D.W., W.Z. and X.J. analyzed the data. D.W., W.Z. and X.J. wrote the paper.

Additional information

Supplementary information accompanies this paper at http://www.nature.com/scientificreports

Competing financial interests: The authors declare no competing financial interests.

How to cite this article: Wang, D. *et al.* Tissue-specific mechanical and geometrical control of cell viability and actin cytoskeleton alignment. *Sci. Rep.* **4**, 6160; DOI:10.1038/srep06160 (2014).